PRACTICAL ASPECTS OF DML-PANEL DESIGN

L Ferekidis, New Transducers Ltd.
email: l.ferekidis@nxtsound.com

1 INTRODUCTION

In recent years an increasing number of companies have adopted DML (Distributed Mode Loudspeaker) technology in their products utilising the properties of this peculiar acoustic transducer. It is the diffuse rather than coherent sound field and the radiation characteristic that distinguishes a DML mostly from pistonic moving transducers.

Given the fact that most lucky engineers started their career working on traditional piston-like moving-coil transducers, they are usually surprised how different it is to develop a DML with distinct requirements. Certain assumptions regarding the way a loudspeaker usually radiates are suddenly turned over. Given a conventional drive unit it can be assumed that at high frequencies an arbitrary off-axis frequency response drops below the on-axis response. This behaviour also known as beaming is determined by the diameter of the radiating area. In contrast to this the high frequency output of a DML can stay constant over a broad radiation range. It may even rise above the on-axis level for a particular angle. A DML does not necessarily have a single, strong, and forward pointing main lobe, therefore the radiation characteristic is of high priority during the design process.

The de-facto standard to display radiation characteristic is the polar plot for a single frequency, an octave band (better), or a 3rd-octave band (even better). Other ways to visualize radiation-data are two- or three dimensional frequency-directivity plots. These are contour-plots of SPL-levels against angle and frequency using cartesian coordinates. The level information is either just colour-coded (2D) or colour- and contour-coded (3D). The main argument against both representations is the amount of information dumped into a single plot. Especially when displaying 2D-plots of DMLs it becomes difficult to judge which peak is perception wise important, not to mention dips, which are easily overlooked. By accumulating the vast amount of measurement data into three acoustic-power responses, a simplified and clear representation has been developed, that enables engineers to spot radiation problems.

2 THE PROBLEM WITH RADIATION DATA

Fig. 1 and Fig. 2 show the 2D-representation of a typical DML and a 2-way loudspeaker while Fig. 3 and Fig. 4 display the same information as 3D-plots. The radiation characteristic of the 2-way system shows a gently changing shape, indicating a good dispersion and only slight tonal changes when moving to larger angles. In contrast to that there are a number of peaks and dips located in the DML's frequency-directivity plot, but it is difficult to judge how they will affect tonality. While the 2D-plot gives a good indication of both peaks and dips, it becomes difficult to even find an appropriate perspective for the 3D-plot in Fig. 3 (upper plot). Due to the peaks some of the local dips are hidden, so that the total image of the DML is distorted.

It can be summarised, that due to the diffuse nature of a DML and the therefore irregular radiation characteristic the 3D-plot is not a suitable representation.

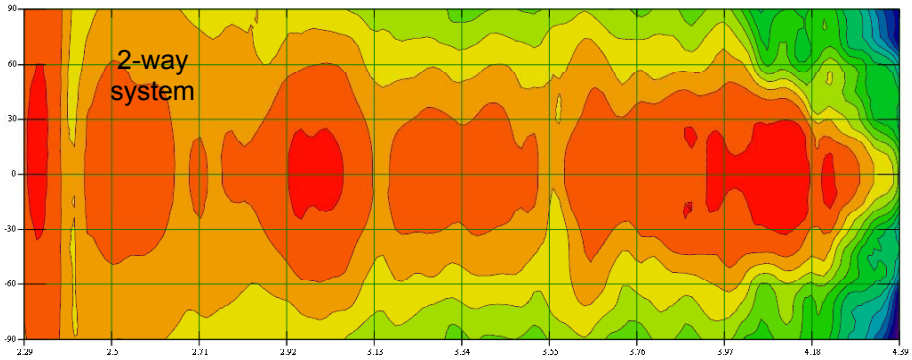

Fig. 1 2D frequency-directivity plot of a 2-way loudspeaker. SPL are colour-coded with 3dB step size. Levels are plotted against log10(f) (x-axis [200Hz-25kHz]) and angle (y-axis [-90°-90°]).

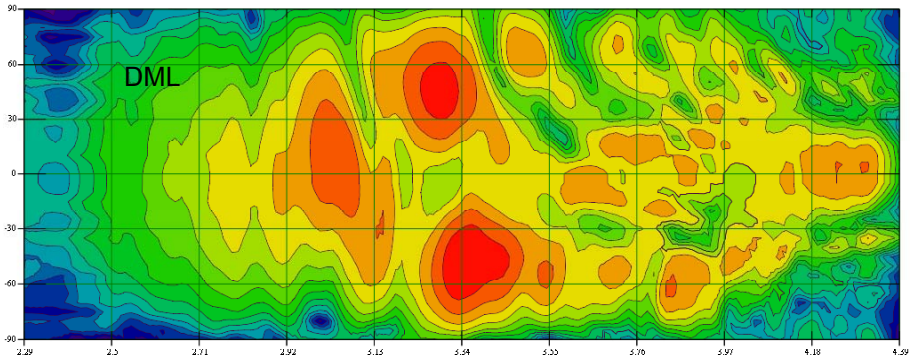

Fig. 2 2D frequency-directivity plot of typical DML. SPL are colour-coded with 3dB step size. Levels are plotted against log10(f) (x-axis [200Hz-25kHz]) and angle (y-axis [-90°-90°]).

Although some of the drawbacks can be overcome when switching to the 2D-plot (peaks hiding valleys) a judgement on the tonal balance of the DML remains difficult. The author's opinion here is, that there is simply too much information squeezed into a single diagram making it difficult to focus on a particular detail. Furthermore the colour coding may indicate the level differences upon a certain frequency range but is not as intuitively judge able as a single frequency response graph.

Since most engineers are used to judging frequency responses the idea is to derive a set of frequency response like graphs from the polar data. The theory behind it and how it is done is described in the next paragraph.

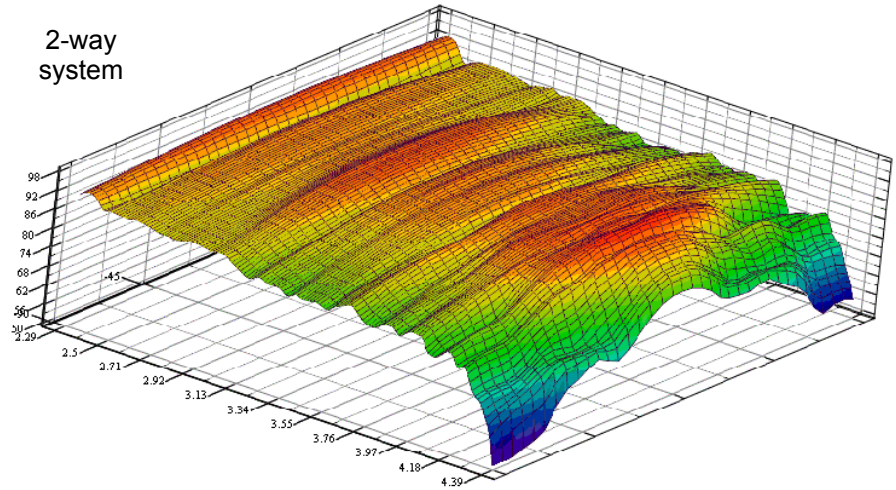

Fig. 3 3D frequency-directivity of same 2-way loudspeaker as in Fig. 1.

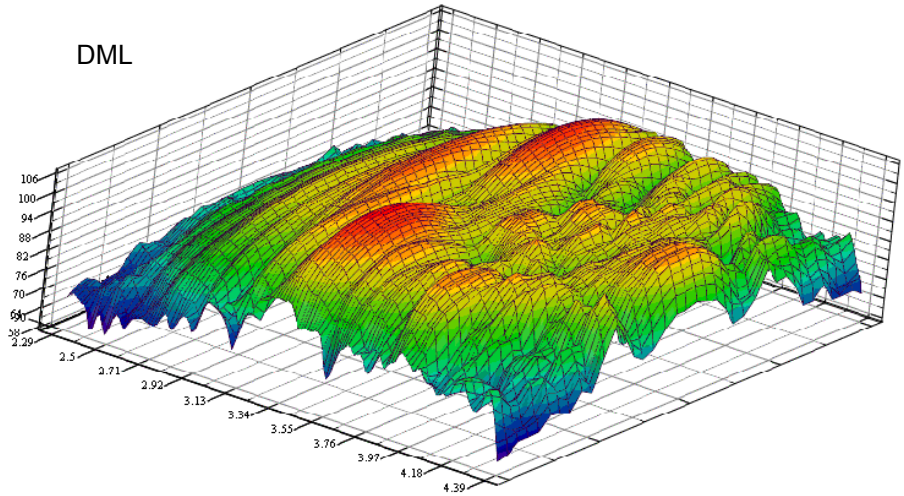

Fig. 4 3D frequency-directivity of same DML as in Fig. 2.

3 THE ART OF SQUEEZING DATA

The task is to find a representation for a given set of measured (polar) data that contains all necessary information in order to closely correlate with the perceived sonic impression. As described in the previous paragraph the attempt to judge all information in one view fails. A short excursion into the fundamentals of information theory shall help to understand why a reduction of information is sensible solution.

3.1 A short survey into Information Theory

According to Fig. 5 information can be split into four sets. The vertical line separates the *redundant* (known) from the *non-redundant* (unknown) part, whereas the horizontal line divides the *relevant* (significant) from the *irrelevant* (insignificant) part. Only the set in the lower right plane (*non-redundant* AND *significant*) contains *interesting information*, since neither *known* nor *insignificant information* would contribute knowledge of interest.

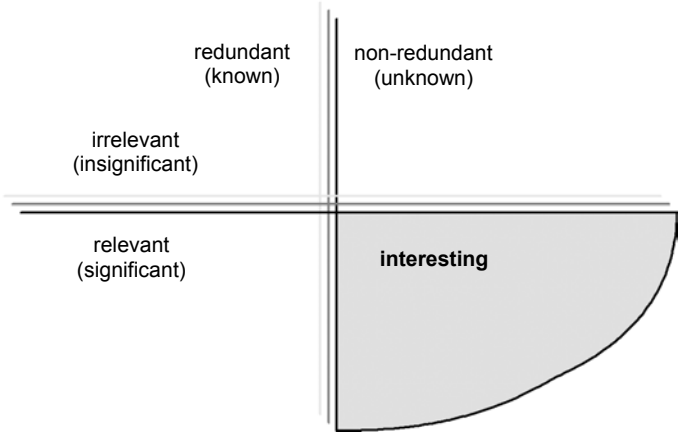

Fig. 5 Plane of information after Schouten

The process of filtering out the *interesting information* (that is, what the engineer needs to get a close correlation between what he measures and what he hears) is subject of the so-called redundancy- and irrelevance-reduction and has led to numerous coding schemes of which MP3 (more precisely MPEG-1 Layer 3) is well known.

To understand redundancy- and irrelevance-reduction in the context of polar data interpretation, the theory is applied to the data of the 2-way loudspeaker (diagrams Fig. 2 and Fig. 4). The fact that the on-axis response curve serves engineers as a reference when designing loudspeakers indicates that it contains most of the *relevant information* they need. Since the radiation is spatially correlated, thus varying slowly as a function of angle, the off-axis responses look very similar. Hence they contain not much *interesting information*. Therefore with a bit of experience (*known information*) the 2D-polar plot contains mostly *redundant* information. Although there is still a bit of *interesting information* (like the "tied-up" region around 4kHz) it becomes *insignificant (irrelevant)* to the engineer.

Applying the same principals onto the DML's polar data (diagrams Fig. 1 and Fig. 3) generates the following string of thoughts. Due to the diffuse radiation of the DML, correlation between measured on-axis response and sonic impression is low. Therefore only a fraction of the *interesting information* is coded in the on-axis response. The peaks and valleys in the 2D-plot indicate diffusivity, a DML-typical characteristic, which, once it is *known*, becomes *redundant*. The precise position of the peaks and valleys are *irrelevant* to the engineer, because of the missing correlation to sonic impression. The task remains to find a coding (processing) scheme that extracts the *interesting information* (those that correlate strongly with the sonic impression) from the polar data of a DML.

3.2 Sound power – the forgotten parameter

In the beginning the logic of Information Theory has a beauty of its own, but when looking for actual coding scheme disillusionment takes over. It does not give many clues as to how to construct them. Fortunately Gontcharov et alteri supply a valuable starting point in their work [1]. When comparing a DML and a 4" cone speaker they conclude that "*for a spatially diffuse radiator, such as a DML, the single point measurement is overly sensitive to small angle fluctuations in the radiation field, and is not representative of the sound output experienced*". They show that the total acoustic power is a more suitable physical measure to characterise a diffuse radiator.

In a nutshell, in the method described below the acoustic power radiated into the frontal hemisphere is divided into three parts, each part representing the acoustic power radiated in a certain direction (back radiation is ignored to simplify the matter). The average sound intensity $\hat{I}_{\alpha\text{-}\beta}$ for an area $A_{\alpha\text{-}\beta}$ drawn between two angles α-β is obtained from the integration of the sound field over this area.

$$\hat{I}_{\alpha-\beta} = \sum_{n \in A_{\alpha-\beta}} \frac{P_n^2}{\rho \cdot c} \tag{1}$$

where P_n are the sound pressures of all measurement points inside $A_{\alpha\text{-}\beta}$, ρ is the density of air, and c the speed of sound. To get the average power $\hat{W}_{\alpha\text{-}\beta}$ each intensity value from (1) is weighted with its associated area $A_{\alpha\text{-}\beta}$

$$\hat{W}_{\alpha-\beta} = A_{\alpha-\beta} \cdot \sum_{n \in A_{\alpha-\beta}} \frac{P_n^2}{\rho \cdot c} \tag{2}$$

In Fig. 6 the areas, which are associated with a string of measurements from a single 2D-measurement, are illustrated. The total acoustic power radiated into the frontal hemisphere is divided into three average powers $\hat{W}_{30}$, $\hat{W}_{30\text{-}60}$, and $\hat{W}_{60\text{-}90}$. Each average power corresponds to a cover-area that draws an angle of 60°.

The average power functions to be calculated are chosen, such that $\hat{W}_{30}$ (red) is representing the power radiated directly towards the listener {[-30°,-30°]}, $\hat{W}_{30\text{-}60}$ (green) representing the power radiated towards primary reflection zones {[-60°,-30°],[30°,60°]}, and $\hat{W}_{60\text{-}90}$ (blue) representing the power radiated elsewhere in the room contributing mainly to the reverberation {[-60°,-90°],[60°,90°]}. This way the contribution of each component to the sonic impression of the DML can be judged independently. Furthermore variations in the average power response like peaks and dips that significantly alter the sound of the DML are exposed. The previously mentioned SPL changes associated with small angle fluctuations are levelled out.

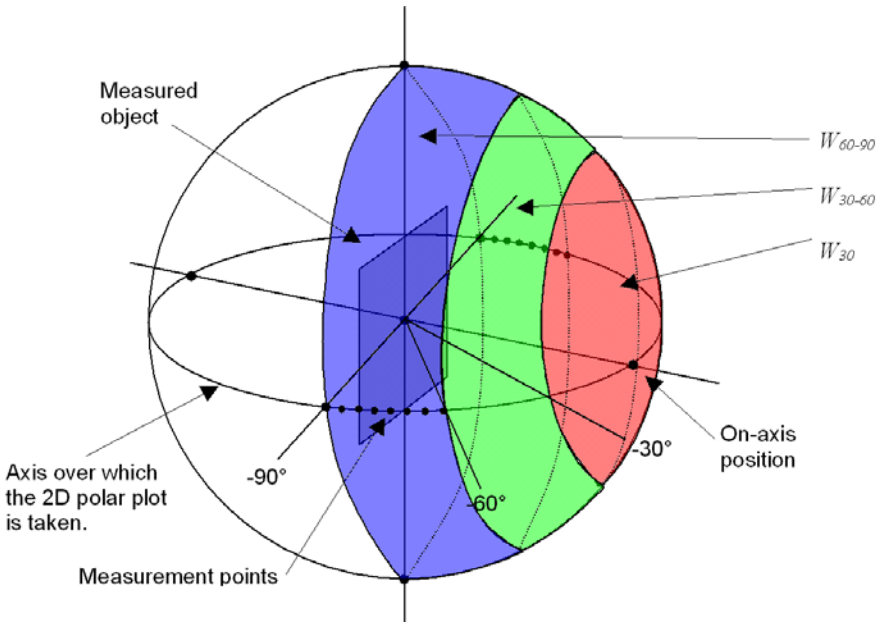

Fig. 6 Illustration of the area associated with a point from a 2D polar plot of the panel, such that the symmetry of the radiation field about the panel axis is used to generate the acoustic power.

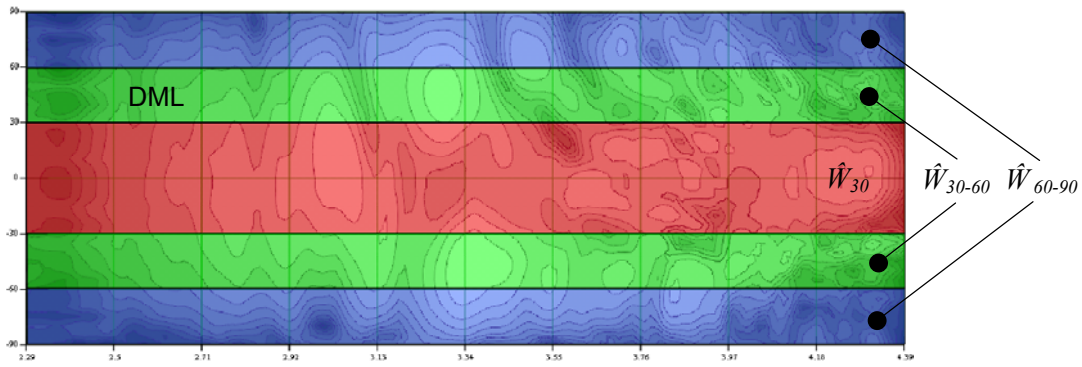

Fig. 7 Projection of the areas illustrated in Fig. 6 on the 2D frequency-directivity plot of the DML in Fig. 2. The average power as a function of frequency is obtained by integrating the measured SPL responses over the indicated angles.

Since all measurements are obtained in the same (horizontal) plane the average sound power functions may only be valid approximations for a small belt along the axis over which the measurements are taken. However, as pointed out in Gontcharov's paper [1], the total acoustic power can be extrapolated sufficiently precise from two full-polar measurements (horizontal & vertical plane).

In Fig. 8 the three average sound power functions $\hat{W}$ are shown for the theoretical case of a monopole and a dipole with $|H(f)_{0°}|=1$. In case of the monopole the average power $\hat{W}$ increases proportional to the associated area $A_{\alpha\text{-}\beta}$ such that $\hat{W}_{60\text{-}90}$ (blue) and $\hat{W}_{30\text{-}60}$ (green) are nearly equal whereas $\hat{W}_{30}$ (red) is down 3dB and 4dB respectively. With the dipole source things get shifted so that $\hat{W}_{30\text{-}60}$ (green) is now equal to $\hat{W}_{30}$ (red) and both are up by 6dB and 7dB respectively compared to $\hat{W}_{60\text{-}90}$ (blue). It should be said that differences of 0.5-1.0 dB are considered to be neglect able perception wise.

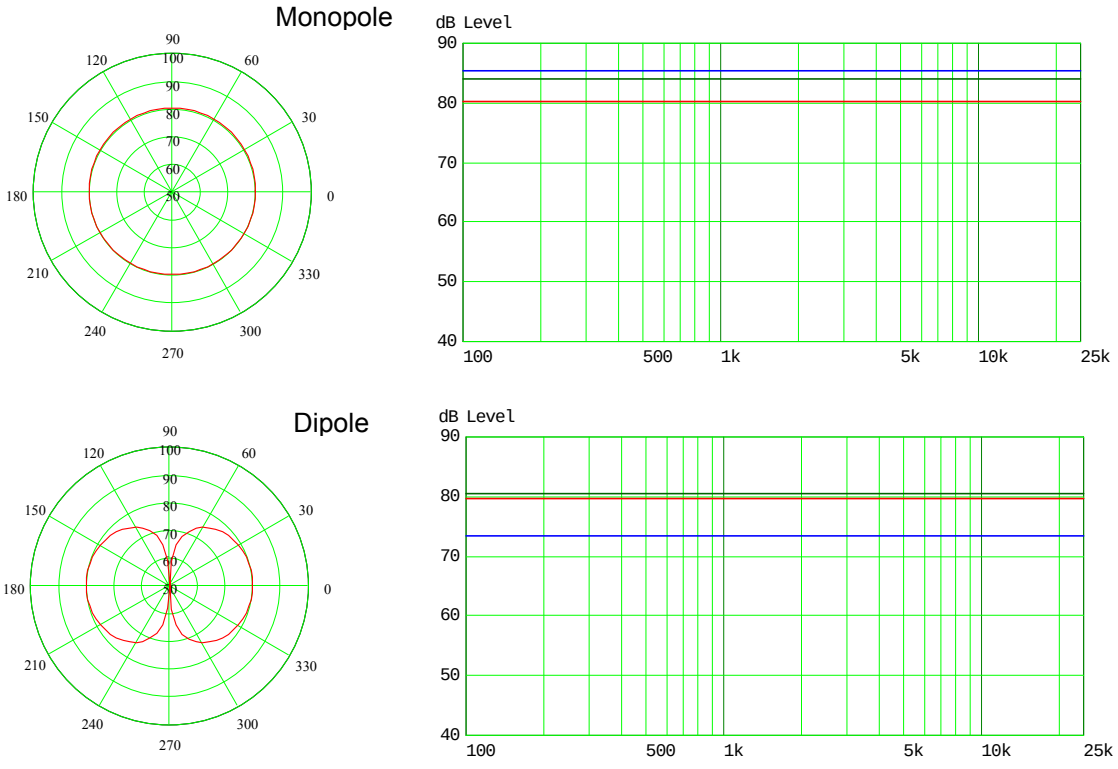

Fig. 8 Average sound power $\hat{W}_{30}$ (red), $\hat{W}_{30\text{-}60}$ (green), and $\hat{W}_{60\text{-}90}$ (blue) plotted for an ideal monopole and dipole.

These somewhat theoretical results are helpful references when judging the average power functions of actual panels. Since all of the examples in the following chapter have been measured as dipoles, e.g. without a back enclosure, it is referred to the traces from Fig. 8 (Dipole) if not stated otherwise.

4 EXAMPLES

Having discussed the somewhat dry theory this chapter should reward the unwavering reader with examples of DMLs to gain some insight in the interpretation of such processed data. In order to simplify the matter all graphs are derived from a single plane measurement taken between -90° and 90° with a 5° resolution. If not explicitly noted the orientation of the measurement plane is horizontal.

4.1 Example 1 – golden ratio panel with two exciters

For those readers who are unfamiliar with the NXT technology a textbook example of DML design is discussed in the following. The simplicity of the design allows for a direct comparison with the dipole example of the previous paragraph.

The dimensions (36x41 cm) are chosen according to the golden ratio (1: 1.134) and the material structure is 100gsm glass-fibre skins on 2.5mm aluminium honeycomb core. Two 19mm-exciters are placed at the so called “recommended exciter positions”. These positions are empirically found to give the smoothest excitation of the first 10-20 modes in panel.

At frequencies below 1.0 kHz the average power traces in Fig. 9 confirm the theoretical results of the dipole in Fig. 8. Above 1.0 kHz the wavelength of the radiated sound wave is already smaller than the width of the panel so that deviations from the theoretical case are expected. While the sound power curve $\hat{W}_{30}$ (radiated to the front) continuously drops with increasing frequency, $\hat{W}_{60\text{-}90}$ (radiated to the side) keeps rising, leaving $\hat{W}_{30\text{-}60}$ (radiated towards the walls) in-between the two graphs above 5.0 kHz. Responsible for this phenomenon is the so-called coincidence effect. Above coincidence the sound propagation in the panel is faster than in air. Depending on stiffness and size of the panel the coincidence effect can cause strong lobes pointing at ±80°. Here the effect acounts for nearly 10dB level difference in the high frequency range.

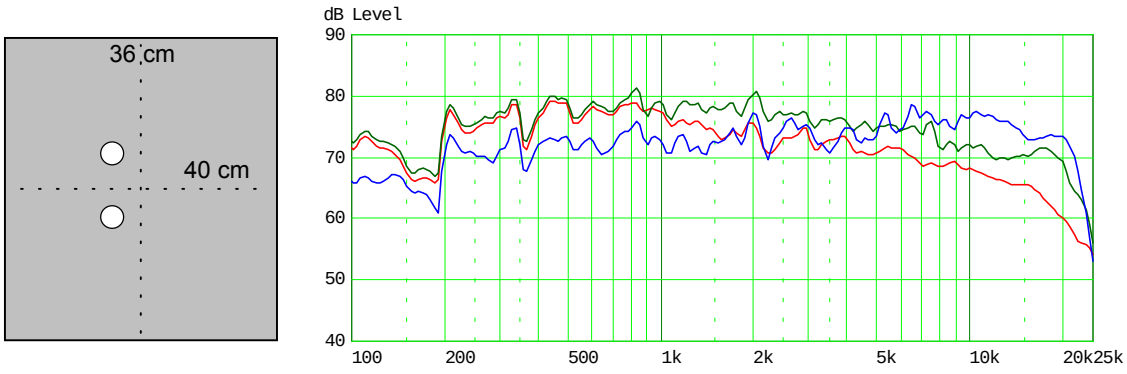

Fig. 9 Example 1. Golden ration panel with 2 exciters. Average sound power $\hat{W}_{30}$ (red), $\hat{W}_{30\text{-}60}$ (green), and $\hat{W}_{60\text{-}90}$ (blue).

Perception wise this might cause some confusion among listeners not familiar with DMLs, since the direct sound contains less high frequency energy than sound bouncing back from the walls. Moreover this unusual distribution of HF-energy also supplies the listener with more information on the sound absorbing characteristic of the listening room. Therefore recent DML designs for HiFi applications aimed at a more focused radiation characteristic at high frequencies.

4.2 Example 2 – golden ratio panel with 1 cluster of 6 exciter

One way of steering the main HF-energy back into the forward direction is to cancel out the unwanted side radiation. Clustering a number of exciters close together can do this. Here six 19mm exciters are arranged in a triangular shaped cluster on the panel from example 1.

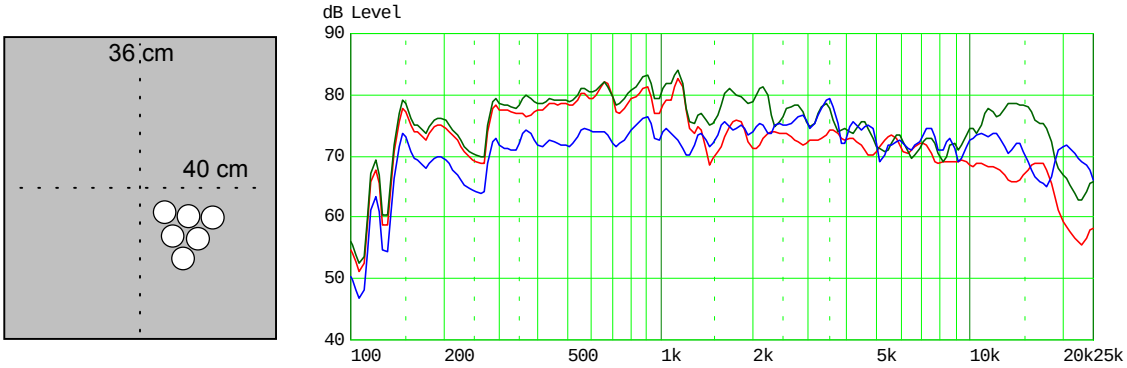

Fig. 10 Example 2. Golden ration panel with 6 exciters in triangular cluster. Average sound power $\hat{W}_{30}$ (red), $\hat{W}_{30\text{-}60}$ (green), and $\hat{W}_{60\text{-}90}$ (blue).

While below 3.0 kHz the graphs in Fig. 10 are unchanged to those in Fig. 9, the level differences between 4.0 and 10.0 kHz disappear. Above 10.0 kHz $\hat{W}_{60\text{-}90}$ and $\hat{W}_{30\text{-}60}$ swap position (compared to Fig. 9) and $\hat{W}_{30}$ rises to the level of $\hat{W}_{60\text{-}90}$. In summary, the maximum HF-energy beamed to the very sides due to the coincidence effect is now radiated towards the primary reflection areas. The amount of HF-energy radiated to the front also increases.

4.3 Example 3 – golden ratio panel with 2 clusters of 3 exciters

We now know the effect of a single large cluster but what about splitting the six exciters into two cluster of three (again, the panel from example 1 is used). The average power graphs for this setup are shown in Fig. 11. When compared to example 2 the frequency range characterised by the strong lobes got shifted from 10.0-20.0 kHz down to 3.0-10.0 kHz. This is due to the larger spacing between the two clusters causing interferences at lower frequencies.

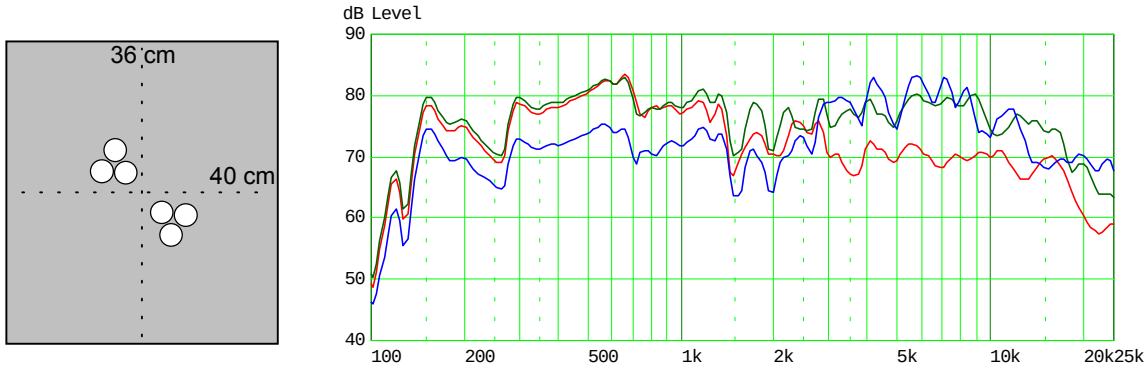

Fig. 11 Example 3. Golden ration panel with 2 triangular shaped clusters of 3 exciters. Average sound power $\hat{W}_{30}$ (red), $\hat{W}_{30\text{-}60}$ (green), and $\hat{W}_{60\text{-}90}$ (blue).

As a result $\hat{W}_{30}$ (radiated to the front) is 7dB down on average in the effected frequency range (3.0-10.0 kHz) compared to $\hat{W}_{30\text{-}60}$ (radiated against the walls) and $\hat{W}_{60\text{-}90}$ (radiated to the sides). Example 3 gives a good demonstration of how the radiation characteristic of a DML can be

manipulated, although the achieved results are inferior to those created by the single, large exciter cluster from example 2.

4.4 Example 4 – long aspect ratio panel with 2 exciters

Long aspect ratio panels are one of these obscure objects that are invented by marketing divisions rather than scientists. While the inferior eigenmode distribution of these panels at low frequencies can be overcome by shifting the crossover higher in frequency, the radiation characteristic can cause severe problems that are easily overlooked when assessing the panel. Therefore the power average functions $\hat{W}_{30}$, $\hat{W}_{30\text{-}60}$, and $\hat{W}_{60\text{-}90}$ are calculated and plotted independently for the horizontal and vertical plane in Fig. 12 and Fig. 13 respectively. Example 4 utilises two closely spaced 25mm exciters. The panel material is carbon fibre skin-layers on a 5mm aluminium honeycomb core.

Due to the short horizontal offset of the two exciters, the off-axis beaming of high frequency energy is prevented (Fig. 12). As a result the average power $\hat{W}_{30}$ (radiated to the front) maintains a higher level at high frequencies than $\hat{W}_{30\text{-}60}$ and $\hat{W}_{60\text{-}90}$. Especially the drop of $\hat{W}_{60\text{-}90}$ (radiated to the sides) indicates that coincidence in the horizontal plane is successfully suppressed. The small width of the panel also helps to reduce horizontal side lobes. On the downside a broad peak around 2.0 kHz can be found in $\hat{W}_{30}$ and $\hat{W}_{30\text{-}60}$ that causes coloration.

The results for the vertical plane measurement in Fig. 13 reveals, that the high frequency behaviour achieved in the horizontal plane cannot be sustained in the vertical plane. Due to the long height of the panel the coincidence effect is strongly developed and pushes $\hat{W}_{30\text{-}60}$ about 5 dB above $\hat{W}_{30}$ in the 3.0 - 15.0 kHz range.

Summing up both results this panel gives a prime example to misguide an engineer. If only $\hat{W}_{30}$ would have been given (e.g. as a result of a special average taken in front of the panel) to judge the performance of the panel, apart from the 2.0kHz peak, no criticism would have arisen. Taking all information into consideration the verdict is different. Now it is revealed that large amounts of mid- and high-frequency energy are actually radiated towards the walls ($\hat{W}_{30\text{-}60} > \hat{W}_{30}$).

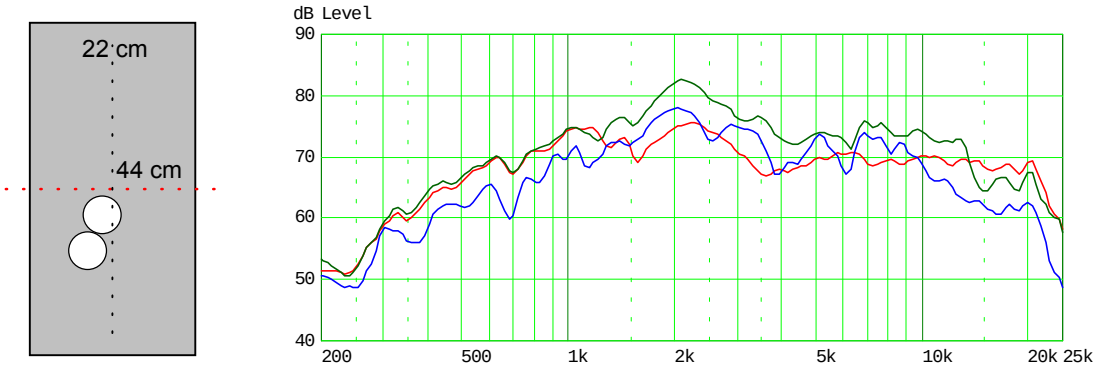

Fig. 12 Example 4. Long aspect ratio panel with 2 exciters. Average sound power $\hat{W}_{30}$ (red), $\hat{W}_{30\text{-}60}$ (green), and $\hat{W}_{60\text{-}90}$ (blue) for **horizontal** plane.

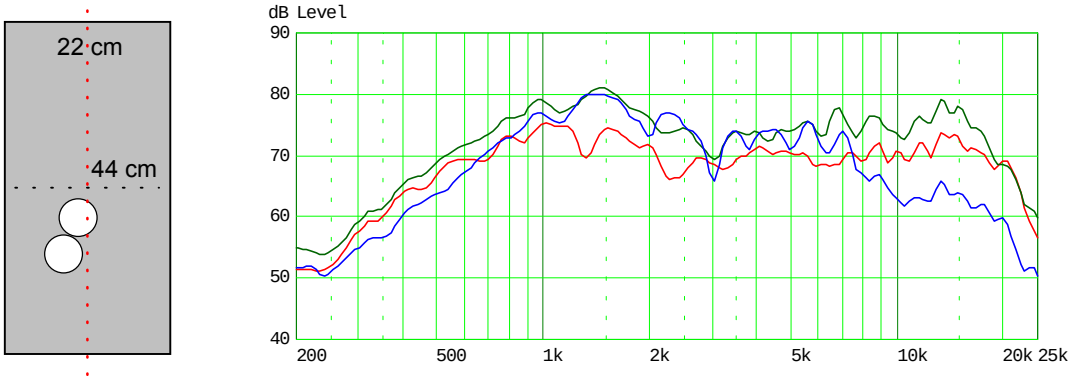

Fig. 13 Example 4. Long aspect ratio panel with 2 exciters. Average sound power $\hat{W}_{30}$ (red), $\hat{W}_{30\text{-}60}$ (green), and $\hat{W}_{60\text{-}90}$ (blue) for **vertical** plane.

4.5 Example 5 – long aspect ratio panel with 4 exciters

In example 2 and 3 it is shown that a single large cluster shows better performance than two smaller clusters of exciters. Although derived for a golden ratio panel this rule might also apply to the long aspect ratio panel of example 4. To answer this question example 5 had been prepared with 2 additional 25mm exciters positioned adjacent to the two initial exciters.

The results of the horizontal plane measurement are shown in Fig. 14. The peak at 2.0 kHz has been smoothed out and $\hat{W}_{30}$ and $\hat{W}_{30\text{-}60}$ are now running well controlled at even level up to 6.0 kHz. The downside of the approach is that $\hat{W}_{30\text{-}60}$ now makes a 5.0-7.0 dB step up between 6.0 and 15.0 kHz. $\hat{W}_{60\text{-}90}$ shows the same step and therefore reinforces this behaviour.

The vertical plane results in Fig. 15 shows $\hat{W}_{30}$ with a similar even graph as for the horizontal plane results in Fig. 14. While in the horizontal plane $\hat{W}_{30\text{-}60}$ is even level up to 6.0 kHz in the vertical plane it becomes even level above 6.0 kHz. Below 6.0 kHz a well controlled but broad peak has developed that reaches up to 10 dB level difference when compared to the on-axis acoustic power $\hat{W}_{30}$. This performance is already problematic because the peak needs to be compensated for. But the worst effect the four-exciter experiment has on $\hat{W}_{60\text{-}90}$. The acoustic power radiated to the side shows the same hump in the graph as $\hat{W}_{30\text{-}60}$ and then quickly decays towards higher frequencies.

Overall the two additional exciters do not improve the acoustic performance of the panel. Reasons are the pronounced frequency range between 2.0 and 5.0 kHz in the vertical plane and the peak between 6.0 and 10.0 kHz in the horizontal plane.

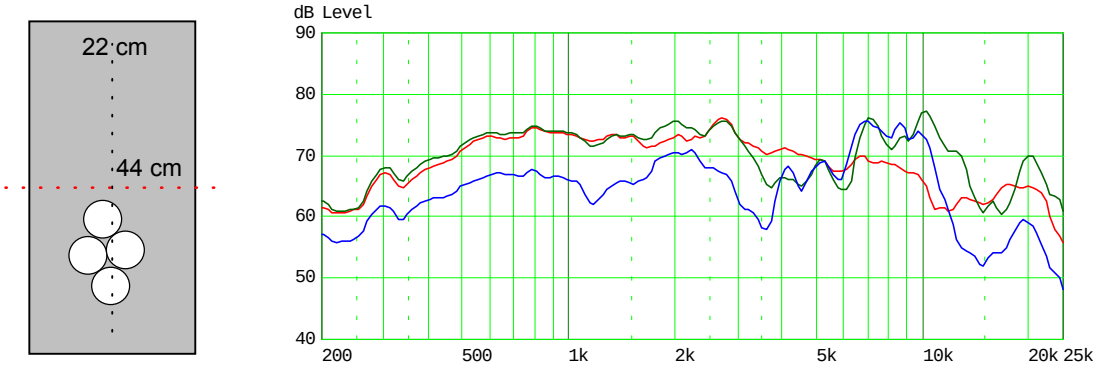

Fig. 14 Example 5. Long aspect ratio panel with 4 exciters. Average sound power $\hat{W}_{30}$ (red), $\hat{W}_{30\text{-}60}$ (green), and $\hat{W}_{60\text{-}90}$ (blue) for **horizontal** plane.

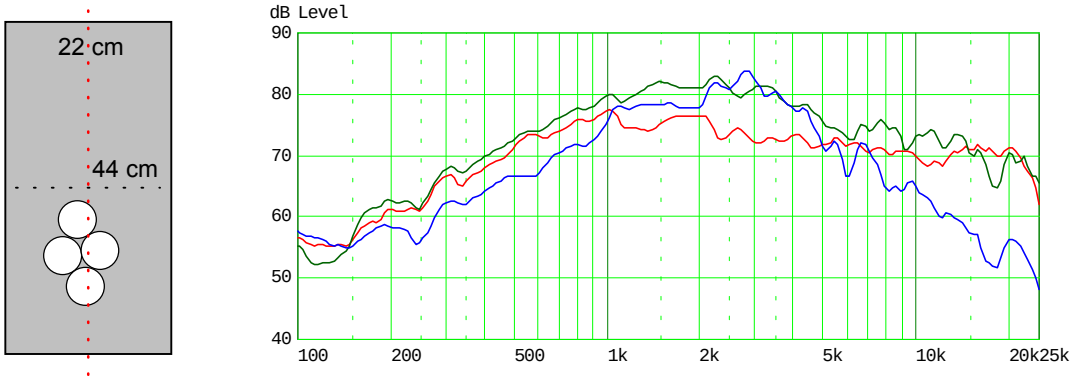

Fig. 15 Example 5. Long aspect ratio panel with 4 exciters. Average sound power $\hat{W}_{30}$ (red), $\hat{W}_{30\text{-}60}$ (green), and $\hat{W}_{60\text{-}90}$ (blue) for **vertical** plane.

As a consequence the coloration added by the floor- and ceiling-reflections differs significantly from the coloration added by the sidewalls-reflections. This causes an acoustic situation that is not in line with most listeners' experiences and will therefore be perceived as disturbing. It is worth noting that this kind of lobbing cannot be mended by the means of equalisation, because it is a direction depending problem.

5 SUMMARY

In this paper the necessity for developing an assessing method for DMLs has been motivated. As a solution the direction depending power average method has been introduced. This method takes the highly diffuse nature of DMLs into consideration and derives three average power graphs, based on a single or dual plane frequency directivity measurement. The graphs plotted in a single diagram create a view that is comparable to SPL graphs. Each graph represents the acoustic power that is radiated into a distinct direction. Each direction is associated with a corresponding propagation path of the energy in the room. The distinguished average acoustic powers are reaching the listener's ear directly, via a primary reflection, or as part of the reverberation in the room. This way a correlation between the calculated graphs and the sonic performance in the room can be achieved.

The proposed method has been applied to 2 different panels with 3 and 2 exciter configurations respectively. On a panel with golden aspect ratio three exciter configurations have been tested. The results show, that the main problem of DML panels are the large portions of mid- and high-frequency acoustic power radiated to the sides. This behaviour is caused by the coincidence effect and becomes more pronounced the larger the panel's dimensions are. It is shown that a cluster of closely spaced exciters can reduce the coincidence effect significantly. The effectiveness of this technique is strongly coupled to the panel size and its material properties. Unfortunately there is no guarantee for success when using exciter clusters. Therefore every design requires careful assessment of the radiation characteristic, but with the proposed method an effective tool is at hand that helps to interpret the sometimes-confusing results of polar measurements.

Finally the author thanks Vladimir Gontcharov for his valuable comments, controversial discussions and patient support on his MathCad-scripts.

6 REFERENCES

[1] V.P. Gontcharov, N.P.R. Hill, V.J. Taylor, "Measurement Aspects of Distributed Mode Loudspeakers", 106th AES Convention, 1999 Munich, Preprint 4970